

Silver nanoparticles prepared from herbal extract of terminalia bellerica for selective detection of mercury ions

Alagan Jeevika¹, Raj Sarika¹, Dhesingh Ravi Shankaran^{1,2,*}

¹Nano-Bio Materials and Sensors Laboratory, PSG Institute of Advanced Studies, Coimbatore 641004, Tamilnadu, India

²National Centre for Nanoscience and Nanotechnology, University of Madras, Guindy Campus, Chennai 600025, Tamilnadu, India

*Corresponding author. Tel: (+91) 44-22202720; Mob: (+91) 9487974004; E-mail: dravishankaran@hotmail.com

Received: 13 January 2016, Revised: 25 February 2016 and Accepted: 22 June 2016

ABSTRACT

In this work, we have investigated the uses of herbal extract of *Terminalia bellerica* (*T.bellerica*) as an efficient reducing as well as capping agent for reliable green synthesis of silver nanoparticles (AgNPs) at room temperature. HR-TEM results of AgNPs confirmed that, the nanoparticles are spherical in shape with an average diameter of $\sim 30 \pm 6$ nm. XRD shows that, AgNPs exhibits the face centered cubic (FCC) structure. AgNPs utilized as a nanosensor probe for detection of mercury ions (Hg^{2+}). AgNPs showed a color change from brownish yellow to colorless on exposed to Hg^{2+} due to the redox reaction of mercury and silver. This sensor probe showed a lower limit of detection of 0.3 ± 0.005 μM . Selectivity of the sensor has been evaluated towards other environmentally heavy metal ions and found that, this sensor is highly selective to Hg^{2+} . AgNPs loaded poly (vinylalcohol) (PVA) films and nanofibers were fabricated by solvent casting and electrospinning methods, respectively. AgNPs loaded PVA films and nanofibers were tested for anti-bacterial studies against *E. coli* and *B. subtilis*. The results indicate that the green synthesized AgNPs possess high microbial activity towards *E.coli*. These AgNPs based functional materials have great potential for application in sensors, anti-microbial coatings, wound dressing and smart textiles. Copyright © 2016 VBRI Press.

Keywords: Green synthesis; AgNPs; *terminalia bellerica*; Hg^{2+} sensor; anti-bacterial activity.

Introduction

Synthesis of silver nanoparticles (AgNPs) using bio-resources has great interest due to the advantages of simple, low-cost and environmental friendly process [1-3]. In general, three green synthesis routes are available to prepare AgNPs, including bacteria, fungi and plant or herbal extract [4 - 6]. Recently, interest has been shown on the synthesis of AgNPs by green route using herbal extract (polyphenols) owing to its wide properties such as anti-oxidant, anti-bacterial and anti-fungal activities. These properties create an ideal coating for biomedical implants. On the other hand, AgNPs also were widely used in various other potential applications like sensors, catalyst, solar cells and opto-electronic devices [7 - 11]. Apart from sensing and electronic applications, it has been known for centuries that silver has bactericidal properties. Silver is a safe and an effective bactericidal metal because it is non-toxic to animal cells and highly toxic to bacteria such as *Escherichia coli* (*E.coli*) and *Staphylococcus aureus* (*S. aureus*) [12]. Silver based compounds have been used in recent years to prevent bacterial growth in medical applications. Especially, colloidal silver (nanosilver) doped polymer fabrics and ceramic materials are used as coating material to prevent the growth of microorganisms [13, 14]. Many studies have been reported on green synthesis of

AgNPs and their microbial activities using potential reductants of plant extracts like *olive leaf* [15], *Datura metel* [16], *Ocimum sanctum* [17], *Adenium obesum* [18], *Iresine herbstii leaf* [19] and *Terminalia chebula* [20]. The present work deals with a simple green synthesis of AgNPs using *Terminalia bellerica* (*T.bellerica*) as a reducing and stabilizing agent at room temperature.

T. bellerica is an herbal medicine, which belongs to the family of *Combretaceae*, commonly known as bahera (In Hindi). *T. bellerica* has green color clustered oval leaves, foul-smelling flowers with brown color and hairy fruit [21, 22]. The major chemical constituents are polyphenols such as gallo-tannic acid, ellagic acid, gallic acid, flavones, chebulaginic acid, beta-sitosterol, mannitol, glucose, fructose and tannins. Among these, tannins are the main constituents of *T.bellerica*. These compounds are the responsible for various activities such as anti-oxidant, anti-microbial, anti-cancer and anti-hypertensive. Both *T.bellerica* and *Terminalia chebula* are used for control of cholesterol and digestive disorders, including diarrhea and indigestion and also been used for HIV infections [23-25]. The fruit also possesses anti-bacterial properties and myocardial depressive activity. These inherent properties make it excellent candidate as reducing and capping agent for the reduction of various metal nanoparticles [24].

Electrospun metal nanoparticles incorporated nanofiber membranes have great potential for wound dressing applications [26]. Nanofibers were produced by electrospinning method. The basic setup of electrospinning has three components: a high power voltage supply, spinneret and collector. In this process, high voltage was given to the dispersed polymer solution with controlled flow rate. The charge repulsion caused between the polymer and the solvent molecules produce forces which are opposite to the surface tension and collected on the surface of the collector. Hence, in the surface of the solution electrostatic force dominates the surface tension of the polymer droplets and thus Taylor cone forms. The nature and morphology of the nanofibers affected by many factors, including the physico-chemical properties of the polymer, electrical conductivity of metal nanoparticles and electrospinning parameters, such as solution viscosity, flow rate, distance between tip to collector and voltage [27-29].

Recently, Nano-composites consisting of metal nanoparticles with the polymer matrix in the form of nanofibers, thin films and hydrogels have great attention in biomedical fields due to different nano-structural dimensions (1D, 2D and 3D) and hydrophilic nature of polymeric network. Especially, nanosilver colloids incorporated with thin film and nanofiber membranes are explored as anti-microbial materials in various biomedical applications, it includes medical textiles, microbial coatings in medical devices, wound dressing materials and cosmetic products [30, 31]. To date, AgNPs have been incorporated into a wide variety of natural or synthetic electrospun nanofibers and as well thin films membranes including curcumin/chitosan/ poly (vinylalcohol) (PVA), chitosan/PVA, chitosan oligosaccharide/PVA, chitosan/PVA/poly ethylene and Gum Karaya/PVA [32-35]. As PVA is a hydrophilic, biocompatible and biodegradable polymer, it is often used in biomedical devices, clothing and household products. Nano-composites are prepared by in-situ preparation method and as well adding the metal nanoparticles into polymer matrix. Recently, Padil *et al.*, [35] reported the synthesis of AgNPs through chemical reduction using the mixture of Gum Karaya/PVA and they showed the anti-bacterial activity of AgNPs 7.9 mm for *E.coli*, 8.0 mm for *P.aeruginosa* and 8.0 mm for *S.aureus*. Moghaddam *et al.*, [36] investigated the in-situ preparation of AgNPs using PANI/PVA composites and reported the anti-bacterial activity of PANI/PVA/Ag nano-composites, which found to be effective for *S.aureus* (15 mm) than *E.coli* (12 mm). Similarly, Abdelgawad *et al.*, [26] prepared AgNPs using chitosan and glucose as reducing agent and spun with PVA polymer and showed anti-bacterial activity against *E.coli* and *S. aureus*.

Mercury is a second highly toxic pollutant (heavy metal ion) in the world and it is widely spread in the all living organisms. Excess consumption of mercury can cause severe health effects to human beings [37, 38]. There are several methods being used for the determination of mercury, it includes atomic absorption/emission/fluorescence (AAS/AES/AFS) [39-41], high-performance liquid chromatography (HPLC) coupled with UV-vis or fluorescence [42], ion selective electrode (ISE), flame

photometry [43] and inductive coupled plasma mass spectrometry (ICPMS) [44, 45]. However, above mentioned methods are more expensive, it needs high vacuum chamber and also time-consuming. Hence, a development of simple, feasible and low-cost determination method for mercury is highly required.

In this work, we have synthesized AgNPs using *T.bellerica* herbal extract at room temperature for the first time with less time. The prepared AgNPs used as a nanosensor probe for colorimetric sensing of mercury ions (Hg^{2+}). AgNPs loaded PVA films and fibers were prepared by solvent casting and electrospinning methods, respectively and they also proved their anti-bacterial activities. This green synthesis can be led to a quick manufacturing method to produce AgNPs for various potential applications like anti-microbial coatings in biomedical devices, smart textiles, chemical sensors and opto-electronic devices.

Experimental

Chemicals details

Silver nitrate (98% ACS grade) was procured from Sigma Aldrich, Bangalore, India. *T.bellerica* seed was purchased from local market in Coimbatore, Tamilnadu, India. Poly (vinyl alcohol) (PVA) were purchased from Himedia. Average molecular weight of PVA is 1,60,000 Da. Metal salts such as $BaCl_2$, $MgCl_2$, $CaCl_2$, $CdCl_2$, $Co(NO_3)_2$, $NiCl_2$, $Cu(CH_3COO)_2$, $Zn(CH_3COO)_2$ and $HgCl_2$ were procured from Merck. Potassium chloride (KCl) was purchased from Rankem. Lead chloride ($PbCl_2$) was obtained from Loba Chemia. The bacteriological media (broth) were obtained from Himedia.

Preparation of aqueous extract of *T. bellerica*

Fruits of *T.bellerica* were collected and cleaned thoroughly, dried and powdered. For the preparation of extract of *T.bellerica*, 1 g of powder was weighed accurately and added into 100 mL of distilled water and kept on stirring at 85 °C for 1 h. Finally, the hot solution was allowed to cool at room temperature and the extract was filtered through the Whatman 40 filter paper. The pure aqueous extract of *T.bellerica* was stored at 10 °C in a refrigerator for further use.

Biosynthesis of AgNPs using *T.bellerica* extract

AgNPs was prepared by green synthesis method using *T.bellerica* as reducing and stabilizing agent. For this experiment, 1 mM of $AgNO_3$ was prepared in 25 mL of distilled water. To this solution, 0.5 mL of freshly prepared aqueous extract of *T.bellerica* was added and kept at room temperature for observation and the formation of nanoparticles was monitored by UV-visible (UV-vis) absorption spectroscopy. After 5 min, the color change was observed from colorless to light brownish yellow color, indicating the formation of AgNPs as well the reduction of silver nitrate through the addition of *T.bellerica* extract. The obtained colloidal nanoparticle was purified by washing three times with water and centrifuged. The supernatant liquid was decanted and the precipitate was redispersed in distilled water.

Nanosensing of Hg^{2+} using biosynthesized AgNPs

The biosynthesized AgNPs was explored as a nanosensor probe for visual sensing of Hg^{2+} . Typically, the stock solution of Hg^{2+} was prepared by calculated amount of mercury salts in aqueous medium. Further dilution of 0.5 mM of the Hg^{2+} was obtained by adding required amount of water to makeup the solutions up to 5 nM. Different concentrations of Hg^{2+} were added to AgNPs and the color change has been observed. In order to study the influence of other heavy metal ions, selectivity study was carried out against various other metal salts such as $BaCl_2$, $MgCl_2$, KCl , $PbCl_2$, $Co(NO_3)_2$, $NiCl_2$, $CdCl_2$, $Cu(CH_3COO)_2$, $Zn(CH_3COO)_2$ and $CaCl_2$ at concentration of 1 mM. All the samples were monitored the color change by visually and UV-vis spectroscopy.

Preparation of AgNPs loaded PVA films

AgNPs loaded PVA films were fabricated by solvent casting method. 5 wt% of PVA solution was prepared by weighing 5 g in 100 mL of distilled water. The previously prepared 1mM of AgNPs was added to the PVA solution and kept on stirring at 65 °C for 2 h to get homogeneous solution. Finally, the obtained solution was poured onto a substrate and casted into a film. Then it was packed at room temperature for the evaporation of the solvent. After that, the dried AgNPs loaded PVA films were peeled-off from the substrate and studied their microbial activities.

Fabrication of AgNPs loaded PVA nanofibers

PVA nanofibers and AgNPs loaded nanofibers were produced by electrospinning method. PVA nanofiber was optimized at the concentration of 12 wt%. For AgNPs loaded PVA nanofiber, *T.bellerica* stabilized AgNPs was added to 12 wt% of PVA polymer solution and kept stirring for 4 h to get homogeneous solution. Then the mixture of solution was spun by electrospinning technique. In the electrospinning process, a high electric potential was applied to the mixture of AgNPs and PVA solution at the tip of the syringe needle. The electrospun nanofibers were collected in the aluminum foil which was placed at the distance of 15 cm from the syringe tip. A voltage of 20 kV was applied to a collecting target by a high voltage power supply. The flow rate of the polymer solution was 0.2 mL/h. Electrospinning was continued for 2 h to form fiber mat.

Anti-microbial activity of AgNPs

AgNPs loaded PVA films, nanofibers and also film of *T.bellerica* were tested for anti-microbial activity by standard agar disc diffusion method against *E.coli* and *B.subtills*. 100 mL of Luria agar was prepared by dissolving 1.3 g of Luria agar in 100 mL of distilled water. The Agar solution was poured in conical flask and plucked with non-adsorbent cotton and sterilized at 120 °C for 20 min. Then, the sterilized media was poured into petridishes and allowed to get solidify. 1 mL of the culture of bacteria was added on the surface and distributed evenly using L rod. Small holes were created on the surface of solidified media using a puncher. Then, prepared films and nanofibers were cut into 1 cm x 1 cm dimension and placed on the punched

site. The covered petridishes were rapped well by paraffin film to seal them. The petriplates were kept in an incubator oven at 37 °C for 24 h.

Characterizations

The formation of AgNPs was monitored by UV-vis absorption spectroscopy using a PG spectrometer, distilled water was used as the solvent. The functional group present in the extract of *T.bellerica* and their responsibility in the synthesis of AgNPs was done by fourier transform infrared (FT-IR) analysis acquired with Shimadzu (Japan), IR Affinity spectrometer in the range of 4000-400 cm^{-1} . The purification of AgNPs was done with help of Sigma 3-30 K high speed cooling centrifuge with the speed of 10,000 rpm with a temperature of 15 °C for 15 min. The morphology and microstructure of biosynthesized AgNPs was examined by high resolution transmission electron microscope (HR-TEM) with help of JEOL JEM-2100 model (Japan). During analysis of HR-TEM, crystalline nature of biosynthesized AgNPs was carried out by selected area electron diffraction (SAED) pattern. For the chemical composition of AgNPs, energy dispersive spectroscopy (EDS) was recorded. The crystal phase structure of biosynthesized AgNPs was studied by powder X-ray diffraction (XRD) performed with PW-6000 X-ray diffractometer (Shimadzu, Japan) operated at 40 kV and 30 mA. For the fabrication of AgNPs loaded PVA nanofibers, home-made electrospinning instrument (PSG IAS) was used. A DM750P Leica polarizing optical microscope was employed for the preliminary studies of PVA and AgNPs loaded PVA nanofibers.

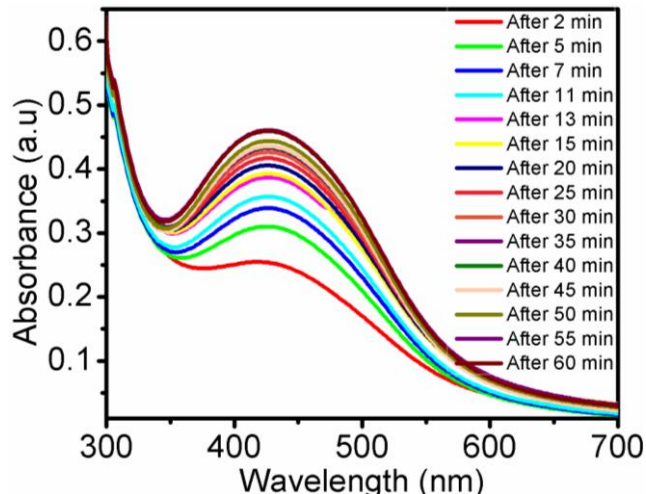


Fig. 1. UV-vis spectra shows effect of time on synthesis of AgNPs using *T.bellerica*

Results and discussion

UV-vis absorption studies

Green synthesis of AgNPs was carried out using herbal extract of *T.bellerica*. Herein, *T.bellerica* extract plays dual role in biosynthesis as reducing as well as stabilizing agent. The mechanism of the reaction involves the reduction of aqueous metal ion in the presence of *T.bellerica* extract. The formation of AgNPs was confirmed by the visible

color change from colorless to brownish yellow color with the addition of *T.bellerica* extract to silver nitrate solution. Further, it was quantitatively monitored by UV-vis spectroscopic studies (Fig. 1). From the Fig. 1 it can be clearly seen that after 5 min, there was a change in the surface plasmon resonance (SPR) absorption of wavelength in the range of 400-500 nm. It can also be observed that, the intensity of the peak was gradually increases with increasing the reaction time, indicating the reduction of Ag^+ to Ag^0 with respect to time. This is due to the formation of AgNPs with the progress of the reaction because the intensity of the SPR is directly proportional to the density of the nanoparticles presented in that solution. It showed a distinct SPR band around 441 nm, indicating the presence of the AgNPs.

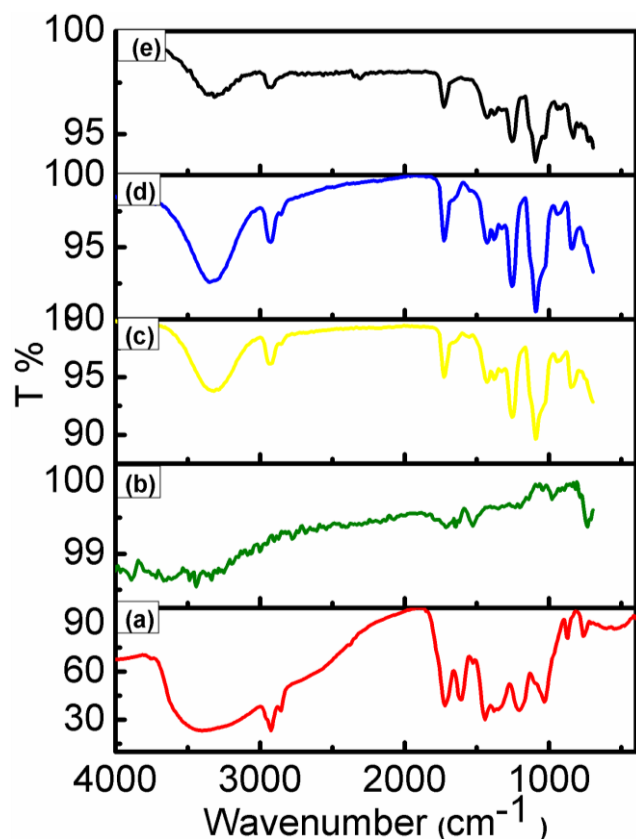


Fig. 2. FT-IR spectra of (a) *T.bellerica* extract (b) *T.bellerica* reduced AgNPs (c) pure PVA film (d) AgNPs loaded PVA film and (e) AgNPs loaded PVA fiber.

FT-IR studies

In order to identify the stabilization of *T.bellerica* on the surface of AgNPs, FT-IR analysis was examined for *T.bellerica* extract and AgNPs. Also, we taken the FT-IR spectra for AgNPs loaded PVA films and nanofibers. FT-IR analysis of *T.bellerica* extract shows strong bands at 3414, 2917, 2846, 1753, 1327 and 1020 cm^{-1} . The bands observed at 3414 and 1753 cm^{-1} correspond to $-\text{OH}$ and $-\text{C}=\text{O}$ stretching modes, respectively. The bands at 1327 and 1020 cm^{-1} were due to the presence of $-\text{C}-\text{O}$ stretching and $-\text{C}-\text{O}-\text{C}$ stretching modes, respectively. The aromatic $-\text{CH}$ was observed as doublet at 2917 and 2846 cm^{-1} . Likewise, FT-IR spectrum of AgNPs shows strong IR

bands at 3428, 1710 and 1040 cm^{-1} which is characteristic nature of $-\text{OH}$, $-\text{C}=\text{O}$ and $-\text{C}-\text{O}-\text{C}$ stretching modes, respectively. From these IR results, confirms the stabilization of biomolecules through the coordination of carbonyl group and oxidized polyphenol onto the surface of the AgNPs. FT-IR spectra of PVA film, AgNPs loaded PVA films and nanofibers were shown in Fig. 2. It shows significant bands at 3315, 2917, 2854, 1427 and 1087 cm^{-1} which indicate the presence of $-\text{OH}$ group from inter and intra molecular hydrogen bonds, $-\text{CH}$ from alkyl groups, $-\text{C}-\text{O}-\text{C}$ group and $-\text{CH}_2$ group, respectively [46]. Also AgNPs loaded films and fiber shows same vibration bands with more intense peak. These results were suggested that there was no interaction between the PVA and AgNPs in addition to that they are physical bound to each other.

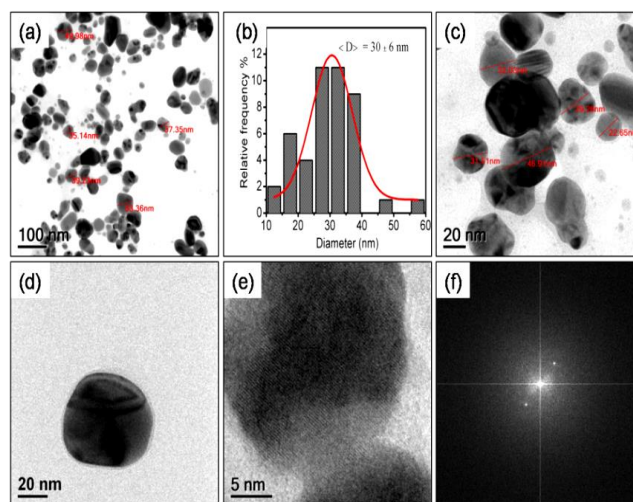


Fig. 3. HR-TEM images of AgNPs at various magnifications (a) TEM image of AgNPs at 100 nm (b) Histogram of statistics relating to the mean diameter of the AgNPs corresponding to image of (a), (c) TEM image of AgNPs at 20 nm (d) TEM image of single AgNPs at 20 nm (e) HR-TEM image of AgNPs at 5 nm and (f) FFT image of AgNPs corresponding to image of (e).

HR-TEM analysis

Fig. 3 depicts the HR-TEM images of biosynthesized AgNPs at various magnifications. For HR-TEM analysis, samples were diluted with distilled water and a drop of solution was deposited on a carbon coated copper grid. The sample was dried in a hot plate, before loading the sample into the samples holder. HR-TEM results, indicates that all the AgNPs are well separated and there is no agglomeration was observed. It shows spherical shape nanoparticles having the diameter in the range of 10-60 nm. The statistics of the mean diameter distribution of AgNPs was given as in Fig. 3(b). It shows the mean diameter of $\sim 30 \pm 6$ nm, which was calculated using image J software. Fig. 3(e) illustrated the HR-TEM image of AgNPs at 5 nm magnifications, it shows the clear lattice fringes that confirms the highly crystalline nature of AgNPs. Further, the fast fourier transform (FFT) image was clearly demonstrated the crystalline nature of Ag atom (Fig. 3(f)).

In order to study the detailed crystal structure of AgNPs, we further performed the SAED and EDS during the analysis of HR-TEM (not given). It exhibited the concentric ring with spot patterns, which are corresponds to the

amorphous and crystalline nature of extract and AgNPs, respectively. It revealed that, the nanoparticles have a lattice d spacing of 2.377 Å, 1.451 Å and 1.232 Å corresponding to the (1 1 1), (2 2 0) and (3 1 1) planes, respectively. All the planes are matching with the d-spacing of (1 1 1), (2 2 0) and (3 1 1) plane of face centered cubic (FCC) of Ag structure from JCPDS 65-2871. Likewise, the EDS of the AgNPs matrix showed the more intense peak observed at 3 Kev for silver atom and confirmed the presence of Ag in the prepared AgNPs.

XRD analysis

In order to study the crystalline phase structure of biosynthesized AgNPs, XRD analysis was carried out. The XRD spectrum of biosynthesized AgNPs was depicted in **Fig. 4**. The diffraction peaks observed at 2 theta values 38.08°, 44.91°, 64.61° and 77.4 ° assigned to (1 1 1), (2 0 0), (2 2 0) and (3 1 1) of lattice plane FCC of silver. The more intense diffraction peak was observed at 38.08° corresponds to the nano-crystalline of silver and also the nanoparticles was grown in the plane of (1 1 1) facets. All the peaks were matches with JCPDS file no 89-3722.

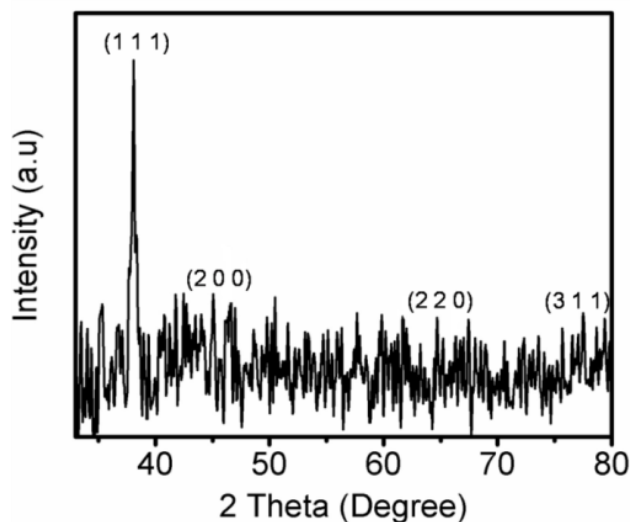


Fig. 4. Powder XRD spectrum of AgNPs.

Colorimetric sensing of Hg²⁺ using biosynthesized AgNPs

Selectivity studies

The tolerance of biogenic stabilized AgNPs for Hg²⁺ over other environmental metal cations were investigated by adding different metal cations to the AgNPs solution and color change has been monitored. **Fig. 5(a)** depicts the photographic image of biogenic stabilized AgNPs in the presence of other different metal ions. From the photographic image, it is clearly seen that, there was no evident color change for any other transition metal cations, except for Hg²⁺. When Hg²⁺ was added to the AgNPs, a significant color change from yellowish brown to colorless was observed due to the redox reaction of silver and mercury and leads to the aggregation of AgNPs. This color change also evidenced by UV-vis spectroscopy by measuring the SPR band absorption of AgNPs. The UV-vis spectra of AgNPs in the presence of different metal cations

were shown in **Fig. 5(b)**. Addition of transition metals to AgNPs, red shifted the SPR absorption peak with broadening was observed. Whereas for Hg²⁺, the SPR band absorption of AgNPs was blue shifted and peak was completely disappeared (441 nm). The tolerance of selectivity bar chart of AgNPs for Hg²⁺ was given in **Fig. 5(c)**. It shows the high selectivity of change in the absorption peak. From the selectivity results we confirmed that, the nanosensor could be able to detect Hg²⁺ highly specifically.

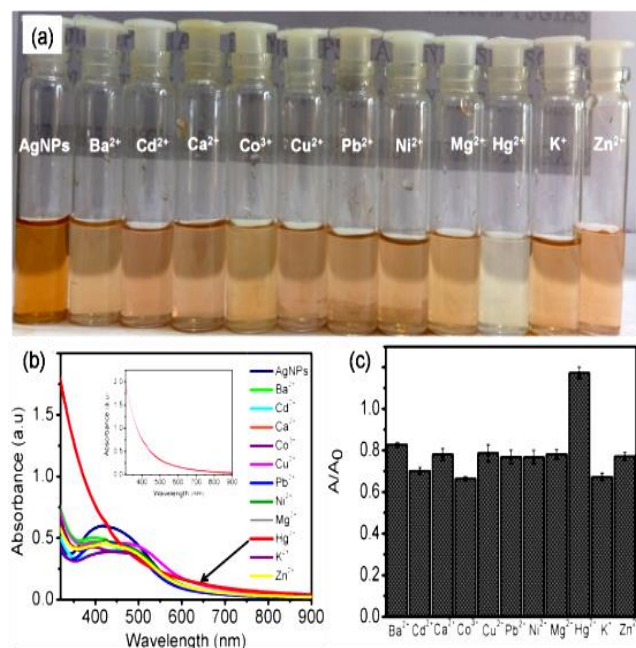


Fig. 5. Selectivity studies: (a) Photographic image showing the selectivity of Hg²⁺ against the different metal cations in the presence of AgNPs, (b) The UV-vis spectra of AgNPs in the presence of different metal cations (c) Bar chart diagram for selectivity of Hg²⁺ against different metal cations; A-is absorbance of AgNPs in the presence of metal cations and A₀-is absorbance of AgNPs at 441 nm.

Sensitivity studies

In order to find out the sensing range of chemosensor, sensitivity studies were carried out. For this experiments, 1 mM of mercury salt solution was prepared and AgNPs was diluted with distilled water, separately. Further, dilution of 0.5 mM of mercury solution was attained by adding calculated amount of distilled water to make up the solution upto 5 nM. Then, 1.5 mL of AgNPs was mixed with 1 mL of different concentrations (5 nM, 50 nM, 0.5 μM, 5 μM, 50 μM, 0.5 mM) of Hg²⁺ solution and final concentration of Hg²⁺ was found to be 2 nM, 20 nM, 0.2 μM, 2 μM, 20 μM and 0.2 mM. When Hg²⁺ added to AgNPs, a significant color change from brownish yellow to colorless was observed due to the redox reaction between silver and mercury with the standard potential of 0.8 V (Ag⁺/Ag⁰) and 0.85 V (Hg²⁺/Hg⁰), respectively [47]. The photographic image of AgNPs in the presence of different concentrations of Hg²⁺ was depicted in **Fig. 6(a)**. From the image, it was clearly seen that, the AgNPs exhibited the sensitivity range upto 2 μM. Further, it was proved using UV-vis spectroscopy by measuring the SPR intensity of AgNPs. The UV-vis spectra of AgNPs in the presence of

different concentrations of Hg^{2+} was given in **Fig. 6(b)**. It was clearly seen from the **Fig. 6(b)**, the absorbance intensity of AgNPs was gradually decreased when increasing the concentration of Hg^{2+} upto 0.5 mM. However, in the case 0.5 mM to 5 μM of Hg^{2+} , there was considerable shift in the SPR peak was observed and also the peak was completely disappeared. This color change from brownish yellow to colorless and change in the SPR intensity of the AgNPs indicate the redox reaction was occurred between silver and mercury and this led to the aggregation followed by the formation of silver and mercury amalgam (Ag/Hg). The absorbance values of AgNPs versus the concentration of Hg^{2+} was plotted, which was shown in **Fig. 6(c)**. It shows a linear relationship ($y = -0.044x + 0.7682$, $R^2 = 0.9987$) between the SPR absorbance of AgNPs at 441nm and Hg^{2+} at concentration from 0.2 mM to 2 μM . The LOD of this sensor system was calculated from the theoretical calculation and found to be $0.3 \pm 0.005 \mu\text{M}$.

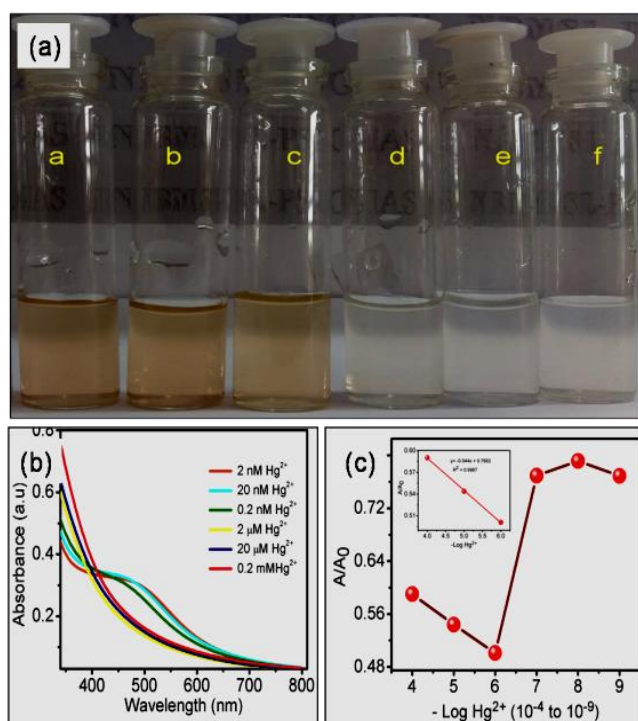


Fig. 6. Sensitivity studies: (a) Photographic image of AgNPs in the presence of different concentrations of Hg^{2+} ; a-5 nM, b-50 nM, c-0.5 μM , d-5 μM , e-50 μM , f-0.5 mM, (b) The UV-vis absorption spectra for response of AgNPs upon addition of different concentrations of Hg^{2+} and (c) Plot of A-absorbance of AgNPs in the presence of Hg^{2+} at 441 nm; A_0 -absorbance of AgNPs at 441 nm.

After sensing of Hg^{2+} , HR-TEM analysis was carried out in order to confirm the redox reaction as well as the aggregation of AgNPs. Hence, the particle size of the AgNPs was increased from 36 nm to 86 nm due to the induced particles aggregation of AgNPs (not given here (see supporting files)). Similarly, EDS spectrum was recorded during the HR-TEM analysis to confirm the presence of mercury in the AgNPs. The EDS spectrum shows the peak for silver and mercury, which indicates after the detection, silver and mercury was present (not given here (see supporting files)) in the solution.

AgNPs loaded PVA films and nanofibers

PVA films and AgNPs loaded PVA films were fabricated by solvent casting method which shows over 95 % of transparency (FT-IR) and good flexibility. Similarly, PVA and AgNPs loaded PVA fiber mat was optimized at the concentration of 12 wt % of PVA solution (see supporting files) by electrospinning method. The diameter of the PVA and AgNPs loaded PVA nanofibers were measured from optical microscope images which shows an average diameter of 522 nm and 444 nm, respectively. From this analysis, we observed that the diameter of AgNPs loaded PVA nanofibers were reduced to 444 nm due to the increased electrical conductivity of AgNPs [30]. In addition to that, the identification and surface morphology of AgNPs loaded PVA fiber was studied by HR-TEM analysis. From the HR-TEM results, it was clearly seen that the nanofibers are smooth and continuous without beads (**Fig. 7(c, d)**). AgNPs observed as dark spots embedded on the surface of the fiber matrix. It shows a diameter of 40 nm dispersed over the PVA nanofiber with an average diameter of $\sim 141 \pm 0.03$ nm.

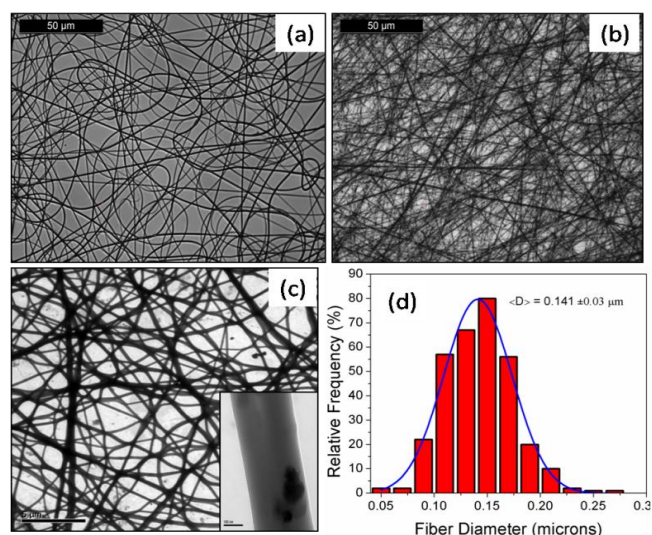


Fig. 7. Optical microscope and HR-TEM images of PVA and AgNPs loaded PVA nanofiber (a) optical microscope image of PVA nanofiber optimized at 12 wt% of polymer solution (b) optical image of AgNPs loaded PVA nanofiber was optimized with the same concentration. (c) TEM image of AgNPs loaded PVA fiber at 5 μm , inset: single nanofiber of AgNPs. The dark spot represented the embedding of AgNPs into the PVA fiber matrix and (d) histogram shows the distribution of fiber diameter.

Anti-microbial activity of PVA films and nanofibers of *T.bellerica* stabilized AgNPs

Anti-microbial activity of AgNPs incorporated PVA films and nanofibers and also *T.bellerica* of films against *B.subtilis* and *E.coli* was studied. The fabricated AgNPs loaded PVA films, nanofibers and *T. bellerica* of films were showed zone of inhibition of 20, 20 and 16 mm, respectively towards *B.subtilis*. Similarly, the AgNPs loaded films, nanofibers and *T.bellerica* films were displays zone of inhibition of 20, 22 and 18 mm against *E.coli*, respectively. From the anti-bacterial activity, it was found that the *T.bellerica* stabilized AgNPs loaded PVA films and

nanofibers exhibits efficient anti-bacterial activity than the *T.bellerica*. Compared to films and nanofibers, nanofibers were showed higher zone of inhibition because of high surface area and porosity nature of the fibers.

Conclusion

In this work, green synthesis of AgNPs was effectively achieved using *T.bellerica* aqueous extract as reducing and stabilizing agent at room temperature, for the first time. HR-TEM results showed spherical shaped nanoparticles with an average diameter of 30 ± 6 nm. The prepared AgNPs exhibited good sensing property towards Hg^{2+} with the limit of detection of 0.3 ± 0.005 μ M. AgNPs loaded films and nanofibers were subjected to anti-microbial studies which showed the excellent microbial activity for AgNPs loaded nanofibers than the films against the *E.coli*. Compared to physical and chemical methods, this protocol is very simple, low-cost, non-toxic and eco-friendly. The AgNPs were free from toxic impurities and could be explored for various applications such as bio-medical coatings, sensors, textile industry and food packing.

Acknowledgements

The authors (A.J. and R.S) would like to acknowledge the PSG son's and charities for providing the PSG IAS fellowship to carry out this work successfully. We also thank Dr. Vasekaran, Department of Animal Biotechnology, Alagappa University for antimicrobial studies.

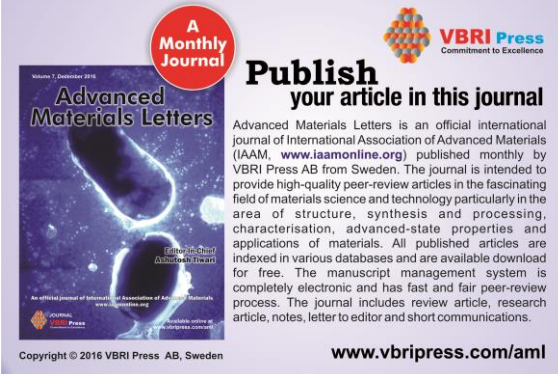
Author's contributions

Conceived the plan: AJ, DRS; Performed the experiments: AJ,SR; Data analysis: AJ, DRS; Wrote the paper: AJ, DRS (AJ, SR, DRS are the initials of authors). Authors have no competing financial interests.

References

1. Das, S.; Das, J.; Samadder, A.; Bhattacharyya, S. S.; Das, D.; Khuda-Bukhsh, A. R. *Colloids Surfaces B Biointerfaces* **2013**, *101*, 325.
DOI: [10.1016/j.colsurfb.2012.07.008](https://doi.org/10.1016/j.colsurfb.2012.07.008)
2. Kaviya, S.; Santhanalakshmi, J.; Viswanathan, B. *Mater. Lett.* **2012**, *67*, 64.
DOI: [10.1016/j.matlet.2011.09.023](https://doi.org/10.1016/j.matlet.2011.09.023)
3. Kavitha, K. S.; Baker, S.; Rakshith, D.; Kavitha, H. U.; C, Y. R. H.; Harini, B. P.; Satish, S. *Int. Res. J. Biol. Sci.*, **2013**, *2*, 66.
4. Korbekandi, H.; Irvani, S <http://www.intechopen.com/books/the-delivery-of-nanoparticles/silver-nanoparticles>.
5. Li, G.; He, D.; Qian, Y.; Guan, B.; Gao, S.; Cui, Y.; Yokoyama, K.; Wang, L. *Int. J. Mol. Sci.*, **2012**, *13*, 466.
DOI: [10.3390/ijms13010466](https://doi.org/10.3390/ijms13010466)
6. Hebbalalu, D.; Lalley, J.; Nadagouda, M. N.; Varma, R. S. **2013**.
DOI: [10.1021/sc4000362](https://doi.org/10.1021/sc4000362)
7. Jeevika, A.; Ravi Shankaran, D. *Colloids Surfaces A Physicochem. Eng. Asp.* **2014**, *461*, 240.
DOI: [10.1016/j.colsurfa.2014.08.002](https://doi.org/10.1016/j.colsurfa.2014.08.002)
8. Chen, L.; Zheng, L.; Lv, Y.; Liu, H.; Wang, G.; Ren, N.; Liu, D.; Wang, J.; Boughton, R. I. *Surf. Coatings Technol.* **2010**, *204* (23), 3871.
DOI: [10.1016/j.surfcoat.2010.05.003](https://doi.org/10.1016/j.surfcoat.2010.05.003)
9. Salman, M.; Iqbal, M.; El Ashry, E. S. H.; Kanwal, S. *Biosens. Bioelectron.* **2012**, *36* (1), 236-241.
DOI: [10.1016/j.bios.2012.04.025](https://doi.org/10.1016/j.bios.2012.04.025)
10. Mathew, T. V.; Kuriakose, S. *Colloids Surfaces B Biointerfaces* **2013**, *101*, 14-18.
DOI: [10.1016/j.colsurfb.2012.05.017](https://doi.org/10.1016/j.colsurfb.2012.05.017)
11. Edison, T. J. I.; Sethuraman, M. G. *Process Biochem.* **2012**, *47*, 1351.
DOI: [10.1016/j.procbio.2012.04.025](https://doi.org/10.1016/j.procbio.2012.04.025)
12. Bowersox, John. Experimental Staph Vaccine Broadly Protective in Animal Studies". NIH. Archived from the original on 5 May 2007. Retrieved 28 July 2007.
13. Cho, J. W.; So, J. H. *Mater. Lett.* **2006**, *60*, 2653.
DOI: [10.1016/j.matlet.2006.01.072](https://doi.org/10.1016/j.matlet.2006.01.072)
14. Montazer, M.; Alimohammadi, F.; Shamei, A.; Rahimi, M. K. *Colloids Surfaces B Biointerfaces* **2012**, *89*, 196.
DOI: [10.1016/j.colsurfb.2011.09.015](https://doi.org/10.1016/j.colsurfb.2011.09.015)
15. Khalil, M. M. H.; Ismail, E. H.; El-Baghdady, K. Z.; Mohamed, D. *Arab. J. Chem.* **2013**.
DOI: [10.1016/j.arabjc.2013.04.007](https://doi.org/10.1016/j.arabjc.2013.04.007)
16. Ojha, A. K.; Rout, J.; Behera, S.; Nayak, P. L. *International Journal of Pharmaceutical Research & Allied Sciences*, **2013**, *2*, 31.
17. Ramteke, C.; Chakrabarti, T.; Sarangi, B. K.; Pandey, R.A. *J. Chem.* **2013**, *2013*, 1
DOI: [10.1155/2013/278925](https://doi.org/10.1155/2013/278925)
18. Li, Y.; Chen, S. M.; Ali, M. A.; AlHemaid, F. M. *Int. J. Electrochem. Sci.* **2013**, *8*, 2691.
19. Dipankar, C.; Murugan, S. *Colloids Surfaces B Biointerfaces* **2012**, *98*, 112.
DOI: [10.1016/j.colsurfb.2012.04.006](https://doi.org/10.1016/j.colsurfb.2012.04.006)
20. Dwivedi, R. *Int. J. Pure App. Biosci.* **2013**, *1*, 1.
21. Kaur, S.; Jaggi, R. K. *Indian J. Exp. Biol.* **2010**, *48*, 925.
22. Kumudhavalli, M. V.; Mohit, V.; Jayakar, B. *Methods* **2010**, *1*, 1.
23. Valli, S.; Shankar, S. G. **2013**, *2*, 154.
24. Elizabeth, K. M. *Indian J. Clin. Biochem.* **2005**, *20*, 150.
25. Molla, M. T. H.; Alam, M.; Islam, M. a-U. *J. Bio-Science* **2009**, *15*, 117.
26. Abdelgawad, A. M.; Hudson, S. M.; Rojas, O. J. *Carbohydr. Polym.* **2014**, *100*, 166.
DOI: [10.1016/j.carbpol.2012.12.043](https://doi.org/10.1016/j.carbpol.2012.12.043)
27. Sirc, J.; Hobzova, R.; Kostina, N.; Širc, J.; Hobzová, R.; Kostina, N.; Munzarová, M.; Jukličková, M.; Lhotka, M.; Kubinová, Š.; Zajícová, A.; Michálek, J. *J. Nanomater.* **2012**, *2012*.
DOI: [10.1155/2012/327369](https://doi.org/10.1155/2012/327369)
28. Kriegel, C.; Arrechi, A.; Kit, K.; McClements, D. J.; Weiss, J. *Crit. Rev. Food Sci. Nutr.* **2008**, *48*, 775.
DOI: [10.1080/10408390802241325](https://doi.org/10.1080/10408390802241325)
29. Zander, N. *Polymers (Basel)*. **2013**, *5*, 19.
DOI: [10.3390/polym5010019](https://doi.org/10.3390/polym5010019)
30. Homaeigohar, S.; Elbahri, M. *Materials (Basel)*. **2014**, *7*, 1017.
DOI: [10.3390/ma7021017](https://doi.org/10.3390/ma7021017)
31. Porel, S.; Ramakrishna, D.; Hariprasad, E.; Gupta, A. D.; Radhakrishnan, T. P. *Chem. synthesis Dyn.* **2011**, *101*, 927.
32. Vimala, K.; Yallapu, M. M.; Varaprasad, K.; Reddy, N. N.; Ravindra, S.; Naidu, N. S.; Raju, K. M. *J. Biomater. Nanobiotechnol.* **2011**, *02*, 55.
DOI: [10.4236/jbnb.2011.21008](https://doi.org/10.4236/jbnb.2011.21008)
33. Li, C. W.; Fu, R. Q.; Yu, C. P.; Li, Z. H.; Guan, H. Y.; Hu, D. Q.; Zhao, D. H.; Lu, L. C. *Int. J. Nanomedicine* **2013**, *8*, 4131.
DOI: [10.2147/IJN.S51679](https://doi.org/10.2147/IJN.S51679)
34. Bayat Tork, M.; Hemmati Nejad, N.; Ghalehbaghi, S.; Bashari, A.; Shakeri-Zadeh, A.; Kamrava, S. *J. Ind. Text.* **2014**.
DOI: [10.1177/1528083714560255](https://doi.org/10.1177/1528083714560255)
35. Padil, T.; Nguyen, N. H. A.; R, A. Š.; Miroslav, H. *J.Nanomaterials*, **2015**, 1-10.
DOI: [10.1155/2015/750726](https://doi.org/10.1155/2015/750726)
36. Ghaffari-Moghaddam, M.; Eslahi, H. *Arab. J. Chem.* **2013**, *7*, 846.
DOI: [10.1016/j.arabjc.2013.11.011](https://doi.org/10.1016/j.arabjc.2013.11.011)
37. Driscoll, C. T.; Mason, R. P.; Chan, H. M.; Jacob, D. J.; Pirrone, N. *Environ. Sci. Technol.* **2013**, *47*, 4967.
DOI: [10.1021/es305071v](https://doi.org/10.1021/es305071v)
38. Li, M.; Wang, Q.; Shi, X.; Hornak, L. a.; Wu, N. *Anal. Chem.* **2011**, *83*, 7061.
DOI: [10.1021/ac2019014](https://doi.org/10.1021/ac2019014)
39. Yang, Q.; Tan, Q.; Zhou, K.; Xu, K.; Hou, X. *J. Anal. At. Spectrom.* **2005**, *20*, 760.
DOI: [10.1039/b505298j](https://doi.org/10.1039/b505298j)
40. Suddendorf, R. F.; Watts, J. O.; Boyer, K. *J. Assoc. Off. Anal. Chem.* **1981**, *64*, 1105.
41. Berzas Nevado, J. J.; Martín-Doimeadios, R. C. R.; Guzmán Bernardo, F. J.; Jiménez Moreno, M. *J. Chromatogr. A* **2005**, *1093*, 21.
DOI: [10.1016/j.chroma.2005.07.054](https://doi.org/10.1016/j.chroma.2005.07.054)

42. Ichinoki, S.; Kitahata, N.; Fujii, Y. *J. Liq. Chromatogr. Relat. Technol.* **2004**, *27*, 1785.
DOI: [10.1081/JLC-120037371](https://doi.org/10.1081/JLC-120037371)
43. Kuswandi, B.; Nuriman; Dam, H. H.; Reinhoudt, D. N.; Verboom, W. *Anal. Chim. Acta* **2007**, *591*, 208.
DOI: [10.1016/j.aca.2007.03.064](https://doi.org/10.1016/j.aca.2007.03.064)
44. Karunasagar, D.; Arunachalam, J.; Gangadharan, S. *J. Anal. At. Spectrom.* **1998**, *13*, 679.
DOI: [10.1039/a802132e](https://doi.org/10.1039/a802132e).
45. Fong, B. M. W.; Siu, T. S.; Lee, J. S. K.; Tam, S. *J. Anal. Toxicol.* **2007**, *31*, 281.
46. Abdelrazek, E. M.; Abdelghany, A.M.; Tarabih, A.E. *RJPBCS*, **2012**, *3*, 448.
47. Farhadi, K.; Forough, M.; Molaei, R.; Hajizadeh, S.; Rafipour, A. *Sensors and Actuators B*, **2012**, *161*, 880.
DOI: [10.1016/j.snb.2011.11.052](https://doi.org/10.1016/j.snb.2011.11.052)



A Monthly Journal

Publish your article in this journal

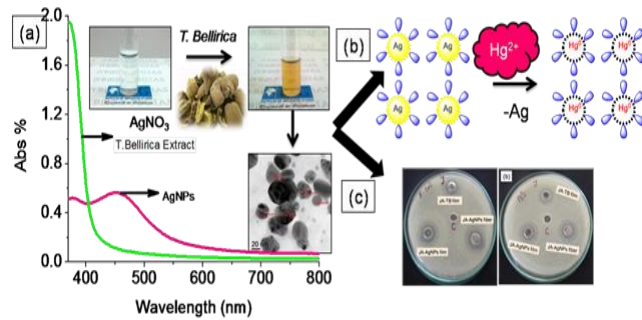
Advanced Materials Letters is an official international journal of International Association of Advanced Materials (IAAM, www.iaamonline.org) published monthly by VBRI Press AB from Sweden. The journal is intended to provide high-quality peer-review articles in the fascinating field of materials science and technology particularly in the area of structure, synthesis and processing, characterisation, advanced-state properties and applications of materials. All published articles are indexed in various databases and are available download for free. The manuscript management system is completely electronic and has fast and fair peer-review process. The journal includes review article, research article, notes, letter to editor and short communications.

www.vbripress.com/aml

Copyright © 2016 VBRI Press AB, Sweden

Supporting information

Green synthesis of AgNPs was effectively achieved using *T.bellerica* aqueous extract as reducing and stabilizing agent at room temperature, for the first time. HR-TEM results showed that spherical shaped nanoparticles with an average diameter of 30 ± 6 nm. AgNPs exhibited good sensor property towards Hg^{2+} . AgNPs loaded films and nanofibers were subjected to antimicrobial studies, which showed the excellent microbial activity for AgNPs loaded nanofibers than the films with against the *E.coli*.



Scheme (a) UV-vis spectrum of *T.bellerica* stabilized AgNPs and their TEM image (b) Colorimetric sensing of mercury (c) Microbial activity of AgNPs

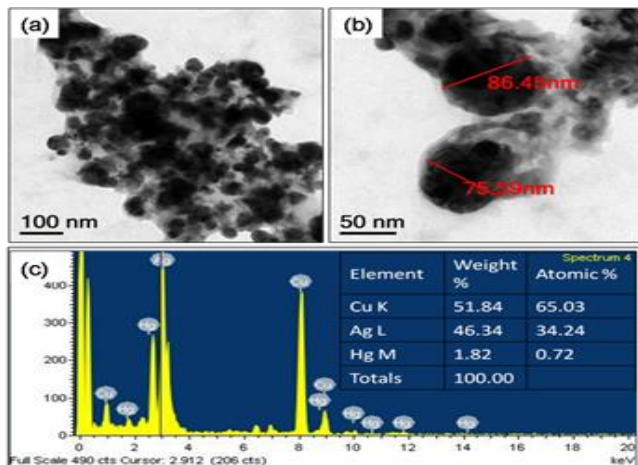


Fig. S1. HR-TEM images of AgNPs in the presence of Hg^{2+} (a) TEM image of AgNPs in the presence of Hg^{2+} at 100 nm (b) TEM image of agglomerated AgNPs containing Hg^{2+} at 50 nm (c) EDS spectrum of AgNPs in the AgNPs in the presence of Hg^{2+} .

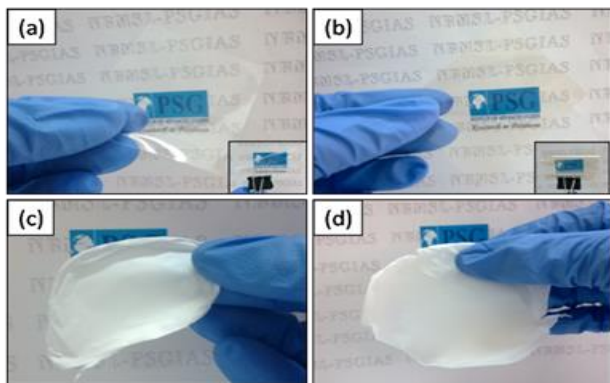


Fig. S2. Fabricated films and nanofibers (a) pure PVA film (b) AgNPs loaded PVA film (c) pure PVA fiber membrane and (d) AgNPs loaded PVA fiber membrane